Supporting Information, ESI†

The use of a sulfonium-based photoacid generator in thiol-ene photopolymers for the controlled activation of transesterification through chemical amplification

Walter Alabiso,[a] Yang Li,[a] Joost Brancart, [b] Guy Van Assche,[b] Elisabeth Rossegger*[a] and Sandra Schlögl*[a]

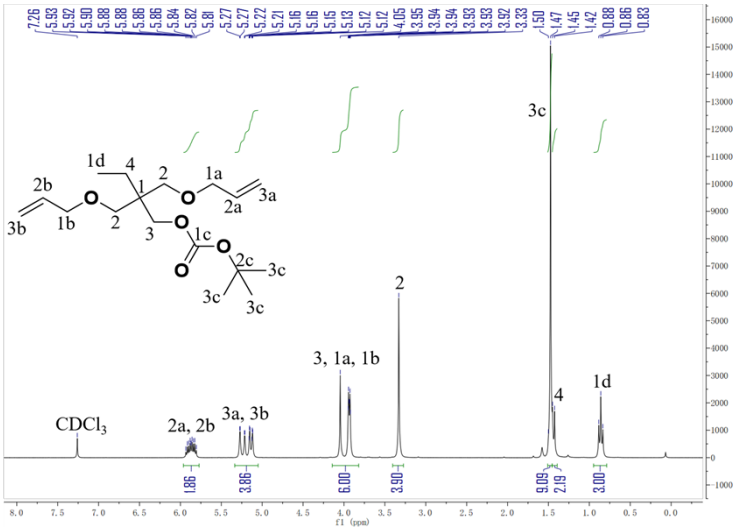

1. Supplementary Figures

Fig. S1 ^{1}H-NMR (300 MHz in $CDCl_3$ at 298 K) of BOC-TMPDE with the characteristic atoms labelled.

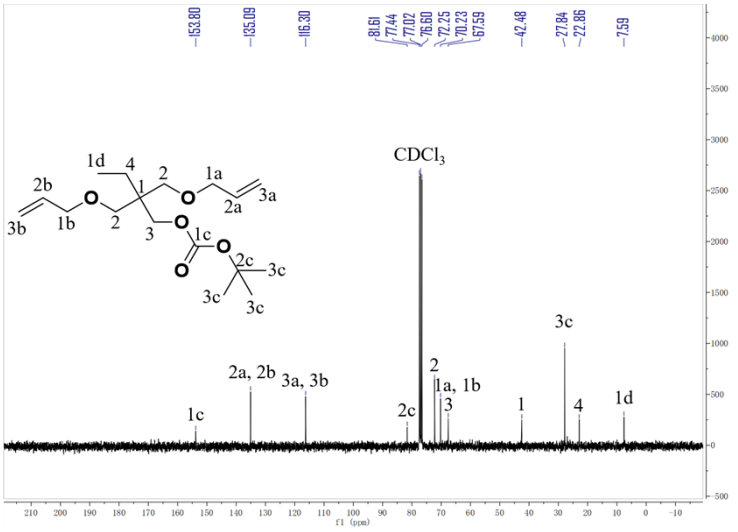

Fig. S2 ^{13}C-NMR (300 MHz in $CDCl_3$ at 298 K) of BOC-TMPDE with the characteristic atoms labelled.

[a.] *Polymer Competence Center Leoben GmbH, Sauraugasse 1, A-8700 Leoben (Austria). E-mail: elisabeth.rossegger@pccl.at, sandra.schloegl@pccl.at*
[b.] *Vrije Universiteit Brussel (VUB), Pleinlaan 2, B-1050 Bruxelles, Belgium.*

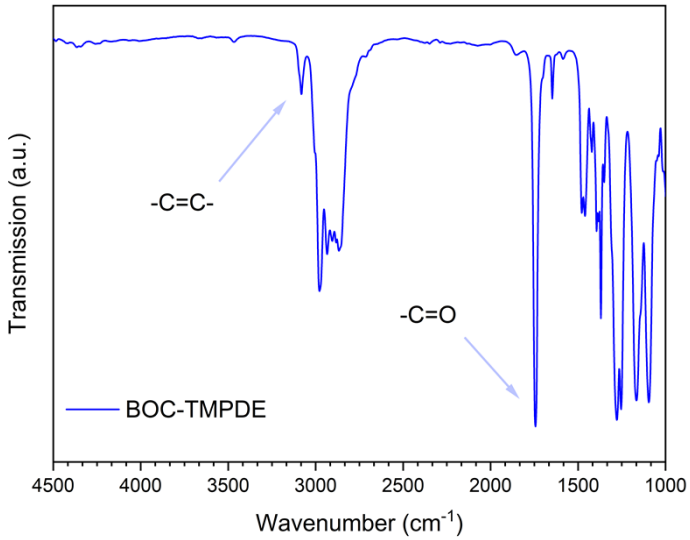

Fig. S3 FTIR spectrum of BOC-TMPDE. The vinyl band at 3082 cm^{-1} and carbonyl band at 1743 cm^{-1} indicate the presence of the *t*-BOC protecting group grafted onto TMPDE.

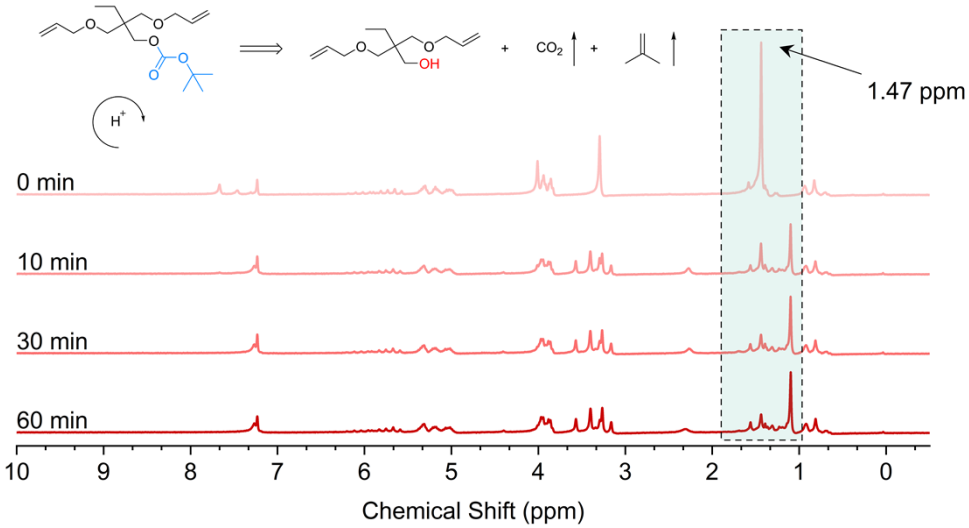

Fig. S4 Deprotection reaction of BOC-TMPDE investigated with ^{1}H-NMR at several irradiation times at 365 nm (44.4 mW cm^{-2}). The decrease in the peak at 1.47 ppm is an indication of the progressive disappearance of the *t*-BOC group, as the activated acid promotes the cleavage reaction (described in the appended scheme).

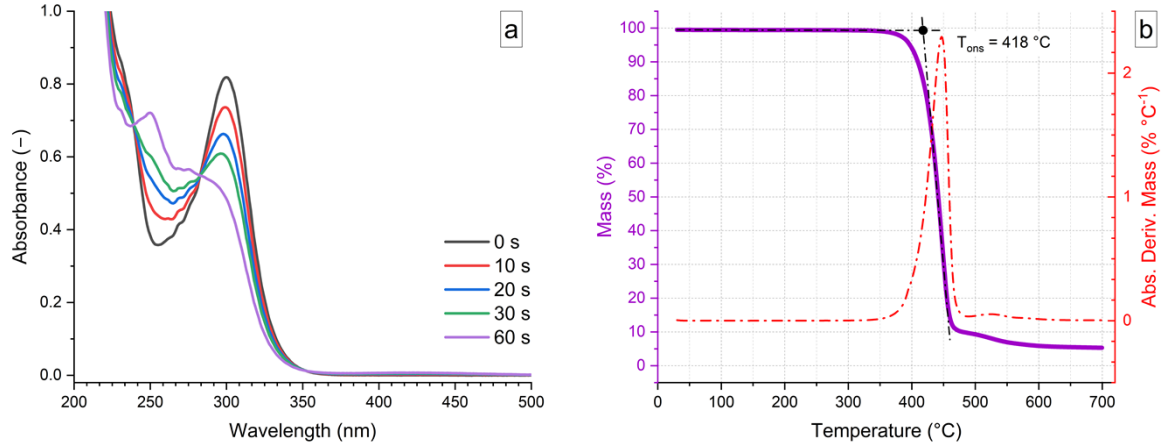

Fig. S5 (a) UV-Vis spectra of the pure 4-phenylthiophenyl-diphenylsulfonium triflate (DPST) in acetonitrile (0.02 mg/mL). (b) TGA of DPST. The compound is thermally stable up to circa 400 °C.

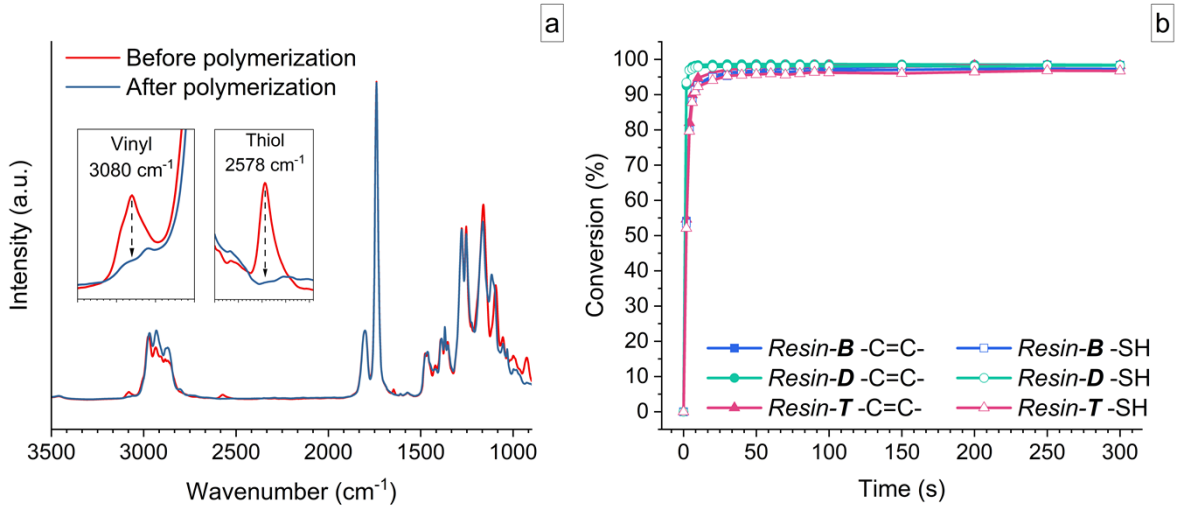

Fig. S6 (a) FTIR-ATR spectra of *Resin-**B*** prior to and after polymerization. The insets magnify the regions of the stretching vibrations of vinyl -C=C- and the -SH thiol. (b) Curing kinetics and final monomer conversions of vinyl groups (full symbols) and thiol groups (open symbols) versus light exposure, as obtained from the change in intensity of the respective FTIR band.

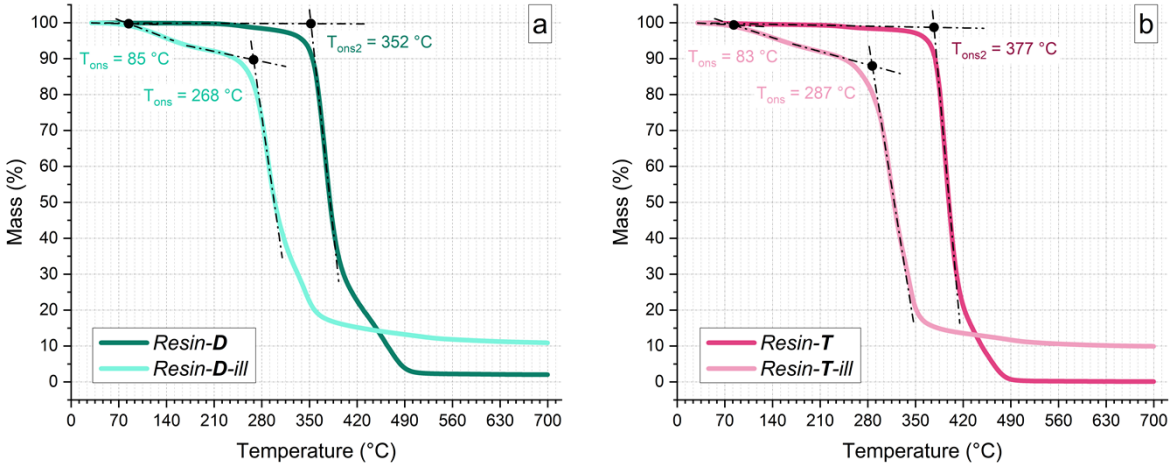

Fig. S7 TGA curves of the reference systems used in this study prior to and after UV illumination. (a) *Resin-**D***, (b) *Resin-**T***. In both cases, the presence of the activated photoacid weakens the thermal stability of the polymer. However, this effect is much more pronounced in *Resin-**D*** due to the lack of -OH groups.

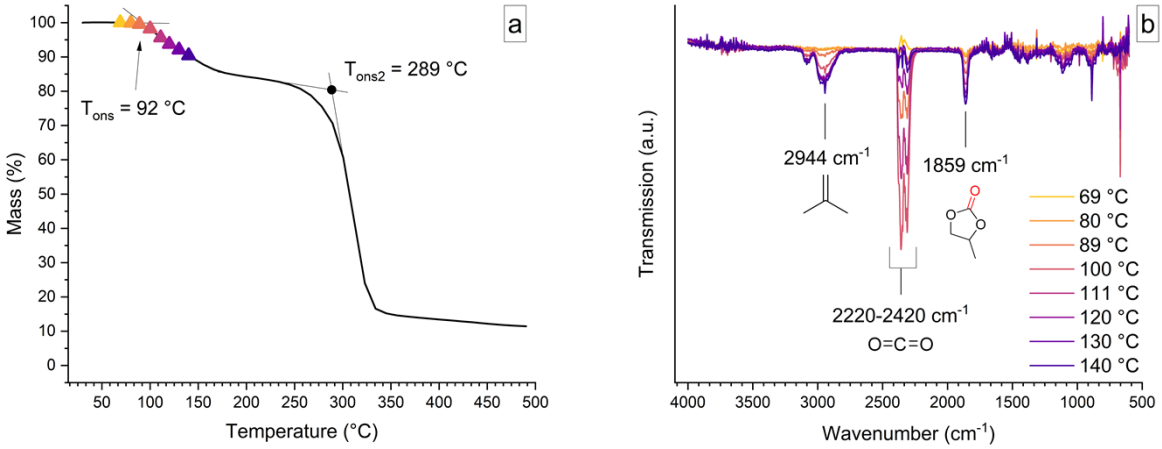

Fig. S8 EGA of *Resin-**B**-non-ill*. (a) Mass loss (%) with a first visible step (92 °C onset of deprotection) and the main network degradation initiating at 289 °C. (b) FTIR-spectra of the gaseous phase acquired at several temperatures. The emission of CO_2 at 2220-2420 cm^{-1} and isobutylene at 2944 cm^{-1} signify that DPST is responsible for gradual deprotection even in its non-activated state. The peak at 1859 cm^{-1} is ascribed to the stretching vibration of the -C=O group present in the solvent (PC).

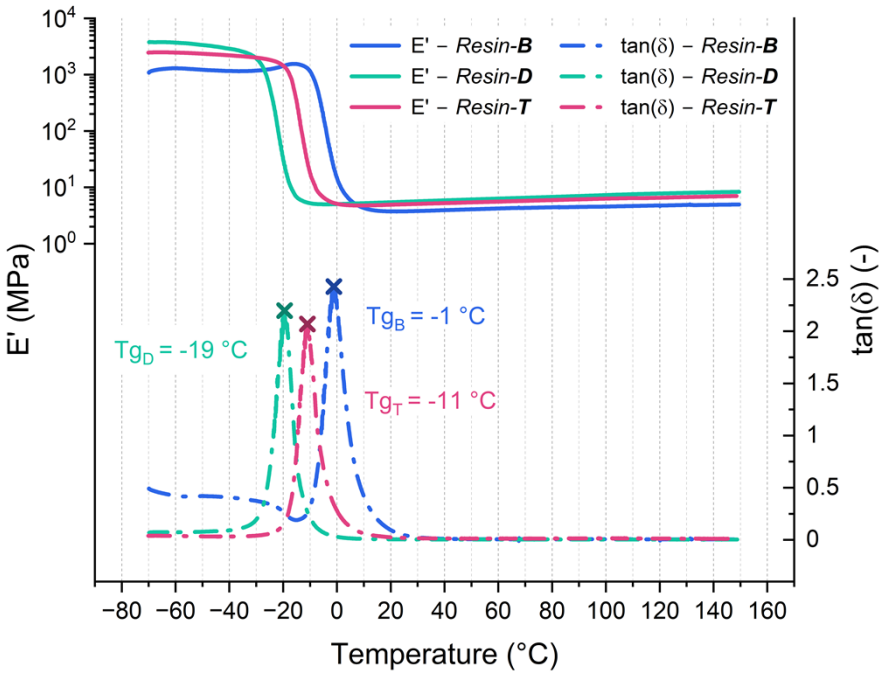

Fig. S9 DMA plot for all the systems analysed in this study in the absence of the photoacid. It is clear that all characterisation experiments were performed above all three glass transition temperatures.

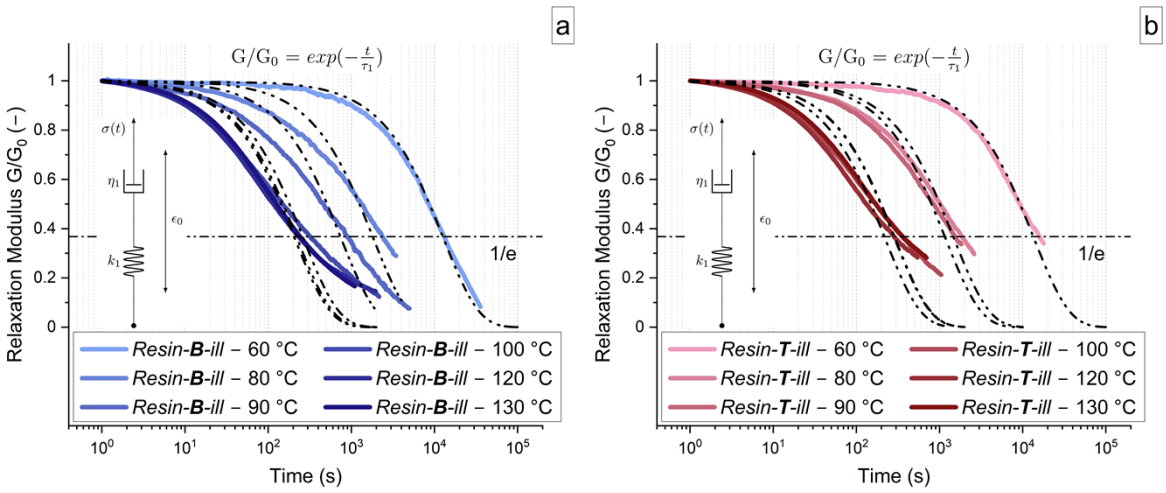

Fig. S10 Rheometer measurements of *Resin-**B**-ill* and *Resin-**T**-ill* fitted with a single exponential equation and its equivalent Maxwell viscoelastic model. (a) Stress relaxation curves of *Resin-**B**-ill* at different temperatures between 60 °C and 130 °C. (b) Stress relaxation curves of *Resin-**T**-ill* at different temperatures between 60 °C and 130 °C. The overall goodness of the fit is really poor, which justifies the use of a double Maxwell model, as described in the paper. The fitting equation acceptably matches only the curves at 60 °C ($R^2 > 0.989$).

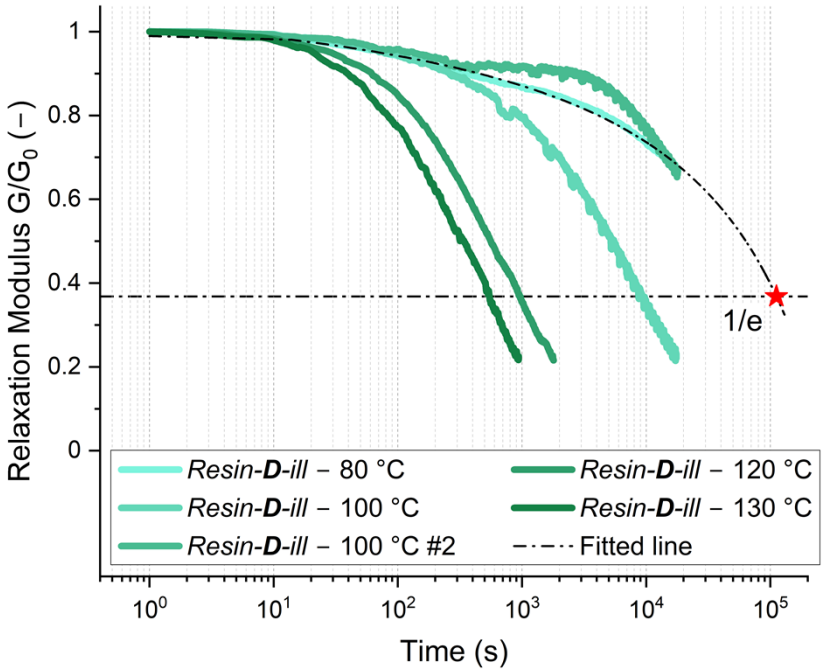

Fig. S11 Rheometer measurements of *Resin-**D***. All samples treated above 100 °C were able to cross the relaxation threshold. The relaxation time of the curve measured at 80 °C was extrapolated via fitting in order to construct an Arrhenius plot (details in Section 2 of ESI†). The sample at 100 °C was measured twice and it showed an inconsistent performance (*Resin-**D**-ill* – 100 °C vs. *Resin-**D**-ill* – 100 °C #2).

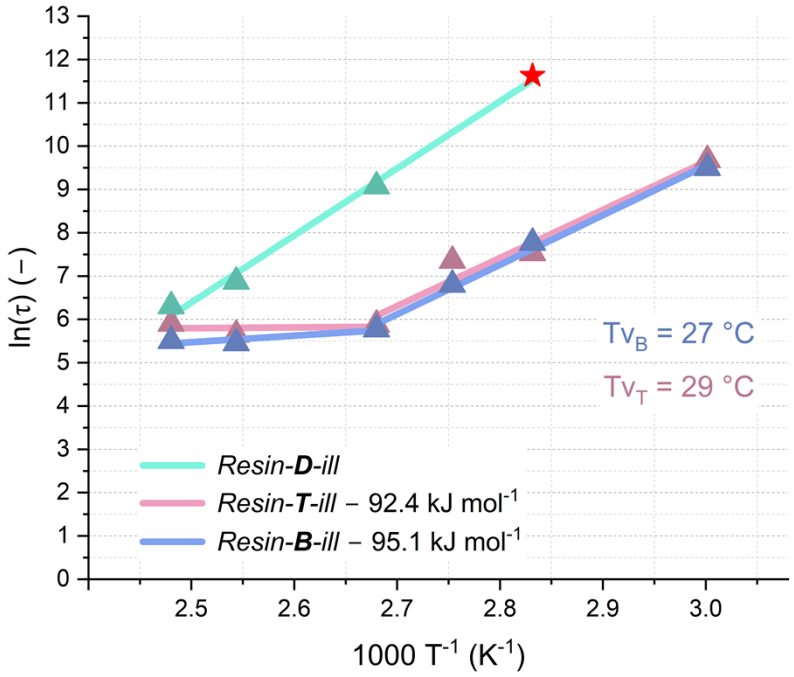

Fig. S12 Complete Arrhenius plot of the illuminated Resin-***D***, -***T*** and -***B***. While the latter two show a corner point (description in the main article), the former fits a linear behaviour.

2. Fitting and Calculations

Modelling the kinetics of stress relaxation with a double Maxwell model

As described in the paper (Fig. 7), *Resin-**B**-ill* and *Resin-**T**-ill* have been modelled following a double Maxwell viscoelastic model, described by the superposition of two phenomena that decay exponentially. The equation used (1.2 in the main text) is presented here once again:

$$G/G_0 = a \cdot e^{-t/\tau_1} + (1-a) \cdot e^{-t/\tau_2} \qquad (1.2)$$

Table S1 and S2 below collect all the fitting parameters determined for the rheometer measurements performed on *Resin-**B**-ill* and *Resin-**T**-ill*.

Table S1 Fitting parameters calculated to fit the double Maxwell model to the rheometer experiments on *Resin-**B**-ill.*

Parameter	Description (unit of measurement)	60 °C	80 °C	90 °C	100 °C	120 °C	130 °C
a	Normalised weight parameter ( )	0.9114	0.7994	0.6320	0.4865	0.3952	0.4530
τ_1	Time constant 1 (s)	14721	2999	1816	1213	1447	936
τ_2	Time constant 2 (s)	1575	138	125	63	69	71
τ_1/τ_2	Ratio. Determines the gap in magnitude ( )	9.3	21.7	14.5	19.4	21.0	13.2
τ_{eff}	Effective relaxation time (s)	13288	2366	898	321	233	245
R^2	Goodness of fit ( )	0.9992	0.9981	0.9972	0.9971	0.9977	0.9992
err_τ_1	Relative error with respect to the equation when τ_1 is used as effective time (%)	+8.86	+20.06	+36.80	+51.35	+60.48	+54.70
err_τ_{eff}	Relative error with respect to the equation when τ_{eff} is used as effective time* (%)	-0.47	+1.26	-4.88	-2.33	+2.89	+0.62

* τ_{eff} was defined in the paper as the time at which the normalised shear modulus of the measured curves reaches 1/e.

It's immediately clear that $\tau_1 \gg \tau_2$ and that the fits are excellent (R^2 > 0.9960, counting the results from Table S2). By substituting both τ_1 and τ_{eff} in equation (1.2) one can calculate the relative error as a deviation from the modulus value 1/e. This justifies the validity of the model in predicting when the curves cross this threshold. However, by substituting τ_1 in (1.2), the curves are far from the relaxation threshold 1/e predicted by a single Maxwell model (a single time constant). This means that τ_1 is not a good candidate for the choice of the effective time τ_{eff} for the subsequent Arrhenius-Rouse model, but it would rather represent an upper bound (all relative errors are positive and much greater than 1). Conversely, determining τ_{eff} by the experimental curves as the value at which the normalised shear modulus crosses 1/e takes τ_2 into account as well.

Table S2 Fitting parameters calculated to fit the double Maxwell model to the rheometer experiments on *Resin-**T**-ill.*

Parameter	Description (unit of measurement)	60 °C	80 °C	90 °C	100 °C	120 °C	130 °C
a	Normalised weight parameter ( )	0.9747	0.7539	0.7705	0.5599	0.5422	0.5365
τ_1	Time constant 1 (s)	14431	2591	2028	930	762	997
τ_2	Time constant 2 (s)	49	224	171	60	55	72
τ_1 / τ_2	Ratio. Determines the gap in magnitude ( )	294.4	11.6	11.8	15.4	13.9	13.8
τ_{eff}	Effective relaxation time (s)	15972	1862	1560	356	283	365
R^2	Goodness of fit ( )	0.9961	0.9978	0.9982	0.9986	0.9994	0.9995
err_τ_1	Relative error with respect to the equation when τ_1 is used as effective time (%)	+2.53	+24.61	+22.95	+44.01	+45.78	+46.35
err_τ_{eff}	Relative error with respect to the equation when τ_{eff} is used as effective time* (%)	+12.40	+0.11	+2.95	-4.06	-2.33	-1.96

For completeness, the parameters deriving from fitting a single exponential Maxwell model (equation and results in Fig. S10) are listed in Table S3 below.

Table S3 Fitting parameters calculated to fit the single Maxwell model to the rheometer experiments on *Resin-**B**-ill* and *Resin-**T**-ill*. Equation and results in Fig. S10.

Parameter	Description (unit of measurement)	60 °C	80 °C	90 °C	100 °C	120 °C	130 °C
			*Resin-**B**-ill*				
τ_1	Time constant 1 (s)	12587	1806	740	260	205	219
R^2	Goodness of fit ( )	0.9950	0.9208	0.9344	0.8782	0.8886	0.9159
			*Resin-**T**-ill*				
τ_1	Time constant 1 (s)	13407	1462	1156	287	217	282
R^2	Goodness of fit ( )	0.9891	0.9498	0.9499	0.8804	0.8972	0.9027

Fitting of the viscoelastic flow kinetics via a Arrhenius-Rouse model

The Arrhenius plots (Fig. 8 in the main text) were fitted in Matlab 2022a with the curve fitting environment activated by the command "cftool". The method used was "NonlinearLeastSquares", "Robust: off", "Algorithm: Trust-region".
To reproduce equation 3 in the main text (below on the left-hand side), the following custom equation (right-hand side) was given as a fitting model:

$$\ln(\tau) = \ln\left(\frac{1}{A_{AR}\cdot C^{b}\exp\left(-\frac{E_a}{RT}\right)} + \frac{1}{A_{RO}\cdot C^{2/3}\cdot T}\right) \quad \longrightarrow \quad y(x) = \ln\left(\frac{1}{a\cdot C^{b}\cdot\exp(-d\cdot x)} + \frac{x}{f\cdot C^{2/3}}\right)$$

Where *y* corresponds to *ln(τ)*, while x replaced *1/T* for simplicity. The results obtained from the curve fitting session using τ_{eff} are collected in Table S4 below.

Table S4 Curve fitting results for the Arrhenius plots of *Resin-**B**-ill* and *Resin-**T**-ill.*

Physical quantity	Physical meaning (unit of measurement)	Corresponding symbol	Value (*Resin-**B**-ill*)	Value (*Resin-**T**-ill*)
A_{AR}	Characteristic constant in the Arrhenius regime (transesterification-limited) (s^{-1})	a	11.34	16.27
C	Catalyst concentration[a] ( )	C	12.39	10.01
b	Exponent of C ( )	b	10.53	11.29
E_a/R	Activation energy over gas constant (slope of Arrhenius line) (K)	d	12.83	12.82
A_{RO}	Characteristic constant in the Rouse regime (diffusion-limited) ($s^{-1}\ K^{-1}$)	f	$2.36 \cdot 10^{-3}$	$1.96 \cdot 10^{-3}$

[a] According to Hubbard et al.[1]

Fitting of the curve "*Resin-D-ill* – 80 °C" in Fig. S11

The curve "*Resin-**D**-ill* – 80 °C" was fitted in Matlab 2022a with the curve fitting environment activated by the command "cftool". The method used was "NonlinearLeastSquares", "Robust: off", "Algorithm: Trust-region".

The following function was implemented:

$$y(w) = \frac{p_1\cdot w^3 + p_2 w^2 + p_3 w + p_4}{w^4 + q_1 w^3 + q_2 w^2 + q_3 w + q_4} \quad ; \quad w = \ln(x)$$

and the following parameters were calculated to yield a fitting curve with $R^2 = 0.827$:

p_1 = -2224
p_2 = $3.001 \cdot 10^4$
p_3 = $-2.605 \cdot 10^4$
p_4 = -6127
q_1 = -1894
q_2 = $2.92 \cdot 10^4$

q_3 = $-2.551 \cdot 10^4$
q_4 = -6191

Calculation of the topological freezing transition temperature (T_v)

The topological freezing transition temperature (T_v) was calculated according to the standard procedure in literature, presented in detail below. From the DMA curves, the average value of the storage Young's modulus (*E'*) for *Resin-**B*** and *-**T*** was taken. Here, as an example, the mathematical procedure for the estimation of T_v in *Resin-**B*** is illustrated below. Assuming incompressibility (Poisson's ratio $\nu = 0.5$) and by exploiting the relation between Young's modulus and shear modulus (*G'*) for elastic linear homogeneous isotropic materials, it follows that:

$$G' = \frac{E'}{2(1+\nu)} = \frac{4.564\ MPa}{2(1+0.5)} = 1.521\ MPa$$

The extrapolated relaxation time τ^* according to Maxwell's model was then obtained, assuming that at $T = T_v$, the viscosity $\eta = 1 \cdot 10^{12}$ Pa·s:

$$\tau^* = \eta / G' = \frac{10^{12}\ Pa \cdot s}{1.521 \cdot 10^6\ Pa} = 6.573 \cdot 10^5\ s$$

T_v can then be extracted from the Arrhenius equation as follows:

$$\ln(\tau^*) = \frac{E_a}{RT_v} + c = \frac{E}{R} \cdot \frac{1000}{T_v} + c \qquad ; \qquad y = m \cdot x + c$$

E/R and *c* are the slope and the y-intercept of the straight line (*i.e.* Arrhenius plot), respectively. After some additional steps, one can calculate the T_v:

$$\frac{1000}{T_v} = \frac{\ln(\tau^*) - c}{m} = \frac{13.40 - (-24.77)}{11.44} = 3.337\ K^{-1} \qquad \Rightarrow \qquad T_v = \frac{1000}{3.337} - 273.15 = 26.5\ °C$$

And the activation energy is:

$$E_a = 1000 \cdot E = 1000 \cdot m \cdot R = 1000 \cdot 11.44\ K \cdot 8.314\ J\ mol^{-1}\ K^{-1} = 95.1\ kJ\ mol^{-1}$$

3. References

[1] A. M. Hubbard, Y. Ren, D. Konkolewicz, A. Sarvestani, C. R. Picu, G. S. Kedziora, A. Roy, V. Varshney and D. Nepal, *ACS Appl. Polym. Mater.,* 2021, **3**, 1756-1766.